Improving FRET Detection in Living Cells

Ching-Wei Chang,[1] Mei Wu,[2, 3]
Sofia D. Merajver[2, 3] and Mary-Ann Mycek[1, 3, 4]

[1]*Department of Biomedical Engineering, University of Michigan, Ann Arbor, MI 48109-2099*
[2]*Department of Internal Medicine, Division of Hematology and Oncology, University of Michigan, Ann Arbor, MI 48109-2099*
[3]*Comprehensive Cancer Center, University of Michigan, Ann Arbor, MI 48109-2099*
[4]*Applied Physics Program, University of Michigan, Ann Arbor, MI 48109-2099*
mycek@umich.edu

Abstract: Unambiguous FRET detection in living cells is often challenging. Here we describe how the advantages of fluorescence lifetime sensing with FLIM, fluorophore selection, and critical environmental controls provide better FRET detection.

OCIS codes: (170.2520) Fluorescence microscopy; (170.6920) Time-resolved imaging.

1. Introduction

Fluorescence resonance energy transfer (FRET) is a quantum mechanical process that involves radiationless energy transfer when two or more fluorophores are present in proximity. It can be used as an *in vivo* nanoscale ruler to detect the distance between fluorophores and the associated interacting proteins to which they are attached [1, 2]. Pioneering studies on FRET were implemented with intensity-based methods [2], such as sensitized emission of acceptor from donor quenching [3, 4] and donor photoquenching with photoactivated acceptor [5].

Fluorescence lifetime imaging microscopy (FLIM) retrieves lifetime data from fluorescence emission. FLIM can be used to detect FRET, because the lifetime of FRET donor is decreased when FRET occurs. FLIM-FRET has some advantages over intensity-based FRET since it is insensitive to artifacts influencing fluorescence intensity, such as optical loss, photobleaching, and difference in fluorophore concentration [6-8].

In this study, we explore the molecular interactions of RhoC (Ras Homology Protein C), which has been found to be a transforming oncogene for mammary epithelial cells and has been identified as a specific marker of aggressive breast cancers. In its active state, RhoC is associated with GTP and localizes to the cell membrane, where it is capable of binding to its effectors and participating in the focal adhesion complex (FAC), to which microtubules converge [9]. When RhoC is inactive, it is associated with GDP and is able to bind with RhoGDIγ (Rho Guanine nucleotide Dissociation Inhibitor gamma) in the cytoplasm. We intend to detect RhoC inactive-form interactions with FRET. The FRET donor was tagged onto RhoGDIγ while the acceptor was tagged onto RhoC.

However, unambiguous FRET detection in living cells can be challenging. The accuracy of live-cell FRET detection can be affected by several factors, such as the method of detection, the choice of fluorophores, and the environment of the cells. In this study, we use FLIM for FRET detection, a better FRET donor, and near-physiological conditions for living cells.

2. Methods

2.1. Fluorescence Lifetime Imaging Microscopy (FLIM)

Fluorescence emission was recorded by gated integration as an approach to measuring the fluorescence lifetime. Using a delay generator, several time gates were utilized to reconstruct the decay curve. Fluorescence decay was

Molecular Imaging II, edited by Kai Licha, Charles P. Lin, Proc. of SPIE-OSA Biomedical Optics,
SPIE Vol. 7370, 737007 · © 2009 SPIE-OSA · CCC code: 1605-7422/09/$18 · doi: 10.1117/12.831718

assumed to be a single exponential and can be characterized by a single number, fluorescence lifetime, which is the time for intensity to drop to e^{-1} of the original value.

To implement time-gated FLIM, recently we have designed and characterized a novel time-domain, wide-field FLIM system for picosecond time-resolved imaging for biological applications [10]. A dye laser pumped by a nitrogen laser for UV-visible-NIR excitation provides a wide-field, less expensive, and potentially portable alternative to multi-photon excitation for sub-nanosecond FLIM of biological specimens [10]. A sample is illuminated by an excitation pulse and the fluorescence emission is recorded by an intensified charge-coupled device (ICCD) camera at a gate delay controlled by the intensifier, with emission intensities integrated during a gate width. This system has a large temporal dynamic range (750 ps – 1 μs), 50 ps lifetime discrimination, and spatial resolution of 1.4 μm, which make it very suitable for studying a variety of endogenous and exogenous fluorophores in biological samples [7, 11, 12]. Fluorescence lifetime maps are determined by first acquiring fluorescence intensity images at four gate delays and then calculating the lifetime values from the intensity decay on a pixel-by-pixel basis (further described below).

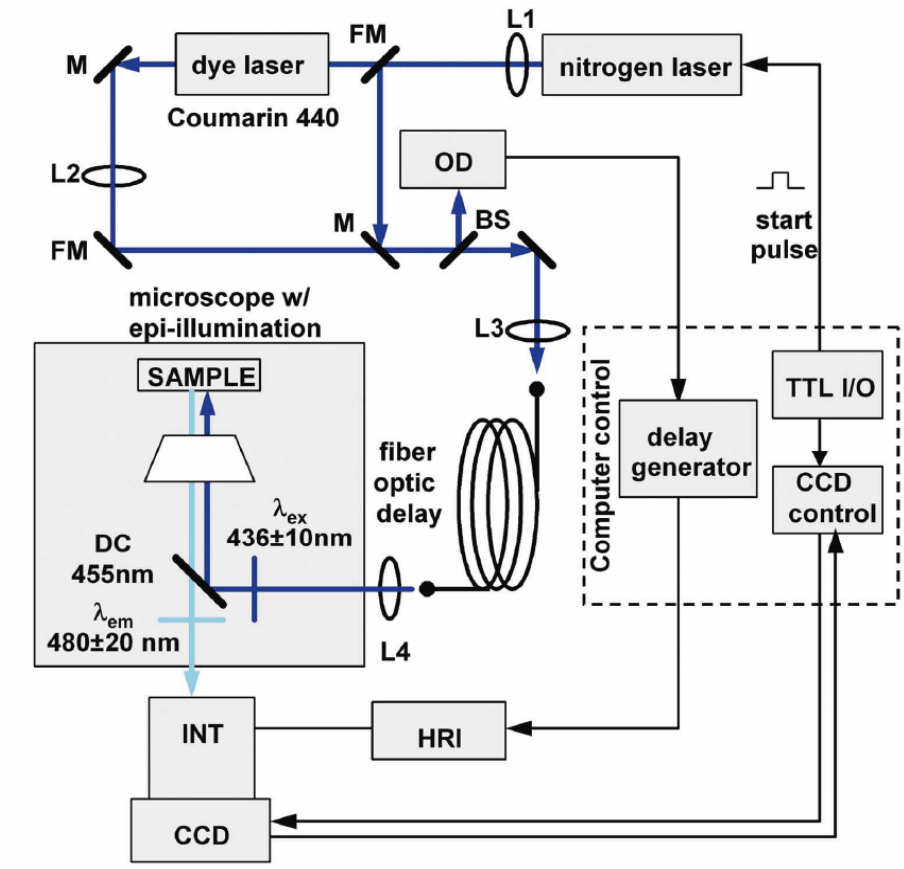

Figure 1 The time-gated FLIM setup used for this study. Abbreviations: CCD = charge-coupled device; HRI = high rate imager; INT = intensifier; TTL I/O = TTL input/output card; OD = optical discriminator; BS = beam splitter; DC = dichroic mirror; FM = "flippable" mirror; L1, L2, L3, L4 = quartz lenses; M = mirror. Thick solid lines = light path; thin solid line = electronic path. [13]

Figure 1 illustrates our FLIM system instrumentation, with some main experimental specifications for imaging living cells described below. The excitation source was composed of a pulsed nitrogen laser (GL-3300, Photon Technology International, Lawrenceville, NJ) pumping a dye laser (GL-301, Photon Technology International, Lawrenceville, NJ), with a wavelength range from UV through near infrared (NIR), depending on the dye in use. An optical fiber (SFS600/660N, Fiberguide Industries, Stirling, NJ) was used to deliver the excitation light to a research-grade, inverted microscope (Axiovert S100 2TV, Zeiss, Germany) in epi-illumination mode. The optical fiber had the added benefit of homogenizing the spatial intensity distribution of the beam. A beam splitter split a reference pulse from the excitation light and sent it to an optical discriminator to generate an electronic pulse, which offered a time reference to a picosecond delay generator (DEL350, Becker & Hickl, Germany), whose output was then used for triggering the gated intensified CCD (ICCD) camera (Picostar HR, LaVision, Germany). The ICCD had variable intensifier gain and gate width settings varying from 200 ps to 10 ms and can be used to implement high-speed imaging in other applications as well [14].

2.2. Lifetime Determination

To creating fluorescence lifetime maps rapidly, a four-gate protocol with a linearized least squares lifetime determination method is used on a pixel-by-pixel basis [15-17]:

$$\tau_p = -\frac{N(\sum t_i^2) - (\sum t_i)^2}{N\sum t_i \ln I_{i,p} - (\sum t_i)(\sum \ln I_{i,p})}$$

where τ_p is the lifetime of pixel p, $I_{i,p}$ is the intensity of pixel p in image i, t_i is the gate delay of image i, and N is the number of images. All sums are over i.

Additional steps in data processing are needed for more accurate lifetime map production. Before lifetime calculation, the step "background subtraction" takes average of the intensities of pixels within a specified background region and subtracts that average value from all pixels. Also, the step "reject" sets intensities to zero for all pixels with intensities below a certain value (assigned as the parameter "reject") after background subtraction. After lifetime calculation, the step "tau range" sets lifetime to zero for all pixels with lifetime above a certain value (assigned as the parameter "taurange") after lifetime calculation, to remove lifetime values in physically meaningless regions. In this study, "reject" was set to 8 and "taurange" was set to 5.

2.3. Sample Preparation

Living monkey kidney epithelial (CV-1) cells were used as our model cells [13]. They were cultured to 60-75% confluency in MEM (CellGro, Mediatech Incorporated, Herndon, VA) supplemented with 10% FBS (Gibco, Invitrogen Corporation, Carlsbad, California) at 37^{o}C under 10% CO_2 before plasmid (a circular DNA used as a vector for gene transfer) transfection with GeneJammer transfection reagent (Stratagene, La Jolla, CA).

2.4. Environmental Controls

In our FLIM system, temperature control is achieved by using Delta T dishes along with a plate heater and an objective heater (Bioptechs, Inc., Butler, Pennsylvania). The CO_2 control is accomplished by using a heated lid (Bioptechs, Inc., Butler, Pennsylvania) to enclose the Delta T dishes, and a peristaltic pump (Model P720, Instech Laboratories, Inc., Plymouth Meeting, Pennsylvania) with adjustable flow rate 0 – 110. The corresponding flow rate with 1/16" inner diameter tubing is 0 – 80 ml/hr, increasing linearly.

2.5. Statistical Analysis

Student's t-tests were used to compare the mean values of lifetimes or intensities of the FRET donors. Homoscedastic t-tests, assuming two-sample equal variance, were utilized because the compared two groups were independent with randomly assigned subjects. Significance level was set to 0.1, although much smaller *p*-values were always acquired when statistical significance was confirmed.

3. Results

3.1. Choice of Fluorophores Can Improve the Consistency of FLIM-FRET Results

The intensity images and lifetime maps of representative CV1 cells transfected with three vector conditions are shown in Figure 2. In this case, Cerulean served as the FRET donor while EYFP was the acceptor. With the same pseudo-color scale, intensity images showed more variability both within and between different vector conditions, while lifetime maps were more uniform and independent of intensity variability. The lifetime values (mean ± standard deviation, in ns) were 2.51 ± 0.18 for cells transfected with Cerulean-RhoGDIγ + EYFP-RhoC, 2.86 ± 0.11 for cells transfected with Cerulean-RhoGDIγ + EYFP, and 2.88 ± 0.17 for cells transfected with Cerulean-RhoGDIγ.. This result indicated that there were molecular interactions between RhoC and RhoGDIγ, with a *p*-value < 1.0e-10.

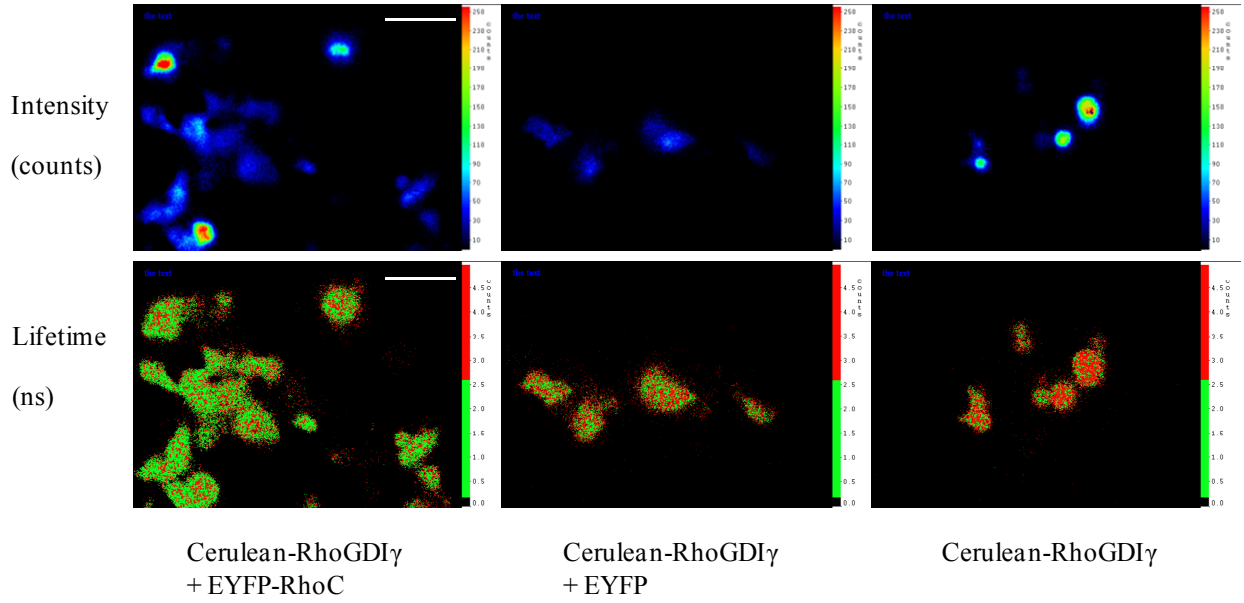

Figure 2 The intensity images and lifetime maps of the CV1 cells transfected with three different vector combinations. In the lifetime maps, the pixels with lifetime longer than 2.6 ns are shown in red; the others are in green. The experimental group exhibits a clearly lower lifetime compared to the two negative controls, and this result suggests the presence of interactions between RhoC and RhoGDIγ. The intensity images, on the other hand, do not clearly suggest such interaction, due to higher inter- and intra-cellular variations. Scale bar = 70 µm.

The above RhoC / RhoGDIγ interaction was more consistently observed with Cerulean in live CV1 cells (such as the results shown in Figure 2) via detection of FRET to EYFP, compared to the common ECFP / EYFP FRET

pair. This consistency was observed in three repeated experiments conducted with independently cultured and transfected sets of cells, in which FRET was detected by comparing the lifetimes of Cerulean. However, when the same experiments were performed with ECFP instead of Cerulean, they did not always provide significant *p*-values for a lower lifetime of ECFP in the ECFP-RhoGDIγ + EYFP-RhoC group versus its negative control (ECFP-RhoGDIγ + EYFP). This result was especially noticeable when the signal-to-noise ratio was low or the number of samples was not high enough.

Cells transfected with only Cerulean-RhoGDIγ do not provide for any random collision of donor and acceptor. Comparison of this negative control with the one that includes an acceptor provides knowledge of not only possible random collisions but also any unexpected binding of acceptor to donor or to donor-bound protein (RhoGDIγ in this case). Comparisons of the two negative controls, Cerulean-RhoGDIγ and Cerulean-RhoGDIγ + EYFP, did not reveal any statistically significant *p*-values, meaning that they were both appropriate negative controls, and that, given our experimental conditions, random EYFP molecules in the cytoplasm did not cause any significant occurrence of non-specific FRET. However, when using ECFP instead of Cerulean in this comparison, some significant *p*-values were obtained against the corresponding null hypotheses, indicating that unwanted interactions or random binding events might have taken place when ECFP served as the donor.

3.2. Environmental Controls Are Necessary for Optimal FLIM-FRET Results

Temperature can affect donor lifetime and the resulting FRET efficiency calculation. To explore the effect of temperature on FRET donor lifetime, we conducted an experiment with one of our negative controls, CV1 cells double-transfected with Cerulean-RhoGDIγ and EYFP. In our results (Figure 3) we observed a shorter lifetime of Cerulean when the temperature was controlled at 37 ^{o}C, as compared to room temperature, with a statistically significant *p*-value (< 1.0e-10). Furthermore, the lifetime difference due to temperature change was also confirmed with CV1 cells transfected with Cerulean-RhoGDIγ only (*p*-value < 1.0e-10). On the other hand, the differences in intensity exhibited large variances and were therefore not statistically significant enough to draw any conclusions.

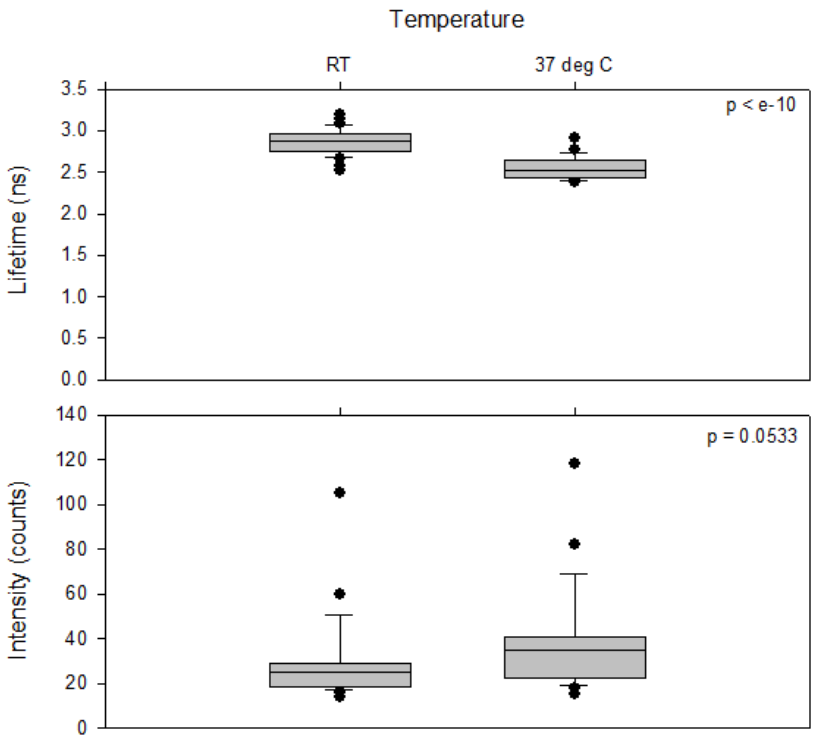

Figure 3 Lifetime and intensity of FRET donor (Cerulean in this case) versus temperature. While the lifetime change due to temperature difference can be clearly observed with a small *p*-value, the differences in intensity exhibited large variances and were therefore not statistically significant enough to draw any conclusions. This lifetime change can therefore be included in later FRET-FLIM measurements. RT = room temperature.

We will be investigating how CO_2 control affects our FLIM-FRET results. Indeed, not only the temperature control demonstrated above, but also CO_2 control should affect fluorophore performance (since they are engineered fluorescent proteins and usually designed to have better translation, folding, and optical properties under physiological conditions), donor lifetime values, degree of molecular interactions reflected by FRET efficiency, and other cellular responses. Our additional studies indicate that further incorporation of CO_2 control can provide better FRET statistics and less non-specific FRET.

As a summary, we have demonstrated (Figure 2) that the imaging of molecular interactions in living cells via FRET can be better detected with FLIM than with intensity, and the consistency of these results can be improved by the use of a better fluorophore, Cerulean. We have also demonstrated that the effect of temperature can be well taken into account in FRET detection with FLIM (Figure 3).

4. References

1. Lippincott-Schwartz, J., E. Snapp, and A. Kenworthy, *Studying protein dynamics in living cells.* Nature Reviews Molecular Cell Biology, 2001. **2**(6): p. 444-456.
2. Schmid, J.A. and H.H. Sitte, *Fluorescence resonance energy transfer in the study of cancer pathways.* Current Opinion in Oncology, 2003. **15**(1): p. 55-64.
3. Chen, Y., M. Elangovan, and A. Periasamy, *FRET data analysis: the algorithm*, in *Molecular imaging*, A. Periasamy and R.N. Day, Editors. 2005, Oxford University Press: New York. p. 126-145.
4. Wallrabe, H. and A. Periasamy, *Imaging protein molecules using FRET and FLIM microscopy.* Curr Opin Biotechnol, 2005. **16**(1): p. 19-27.
5. Demarco, I.A., et al., *Monitoring dynamic protein interactions with photoquenching FRET.* Nature Methods, 2006. **3**(7): p. 519-524.

6. Chen, Y., J.D. Mills, and A. Periasamy, *Protein localization in living cells and tissues using FRET and FLIM.* Differentiation, 2003. **71**(9-10): p. 528-541.
7. Urayama, P.K. and M.A. Mycek, *Fluorescence lifetime imaging microscopy of endogenous biological fluorescence*, in *Handbook of Biomedical Fluorescence*, M.A. Mycek and B.W. Pogue, Editors. 2003, Marcel Dekker, Inc.: New York.
8. Chang, C.W., D. Sud, and M.A. Mycek, *Fluorescence lifetime imaging microscopy.* Methods Cell Biol, 2007. **81**: p. 495-524.
9. van Golen, K.L., et al., *RhoC GTPase, a novel transforming oncogene for human mammary epithelial cells that partially recapitulates the inflammatory breast cancer phenotype.* Cancer Research, 2000. **60**(20): p. 5832-5838.
10. Urayama, P., et al., *A UV-visible-NIR fluorescence lifetime imaging microscope for laser-based biological sensing with picosecond resolution.* Applied Physics B-Lasers and Optics, 2003. **76**(5): p. 483-496.
11. Urayama, P.K., et al. *A UV fluorescence lifetime imaging microscope to probe endogenous cellular fluorescence*. in *Conference on Lasers and Electro-Optics*. 2002: Optical Society of America, Washington D.C.
12. Zhong, W., P. Urayama, and M.-A. Mycek, *Imaging fluorescence lifetime modulation of a ruthenium-based dye in living cells: the potential for oxygen sensing.* Journal of Physics D: Applied Physics, 2003. **36**(14): p. 1689-1695.
13. Zhong, W., et al., *Picosecond-resolution fluorescence lifetime imaging microscopy: a useful tool for sensing molecular interactions in vivo via FRET.* Optics Express, 2007. **15**(26): p. 18220-18235.
14. Xu, Z., et al., *High speed imaging of bubble clouds generated in pulsed ultrasound cavitational therapy-histotripsy.* Ieee Transactions on Ultrasonics Ferroelectrics and Frequency Control, 2007. **54**(10): p. 2091-2101.
15. Bugiel, I., K. König, and H. Wabnitz, *Investigation of cell by fluorescence laser scanning microscopy with subnanosecond time resolution.* Lasers in the Life Sciences, 1989. **3**(1): p. 47-53.
16. Wang, X.F., et al., *A two-dimensional fluorescence lifetime imaging system using a gated image intensifier.* Applied Spectroscopy, 1991. **45**(3): p. 360-366.
17. Sharman, K.K., et al., *Error analysis of the rapid lifetime determination method for double-exponential decays and new windowing schemes*. Analytical Chemistry, 1999. **71**(5): p. 947-952.